Reflection Factor of Gradual-Transition Absorbers for Electromagnetic and Acoustic Waves*

KLAUS WALTHER†

Summary—**Absorbers for electromagnetic or acoustic waves are described, for which a good impedance match and low reflection factor can be achieved by providing a gradual transition of material constants into the lossy medium. The reflection factor can be calculated by means of a Riccati-differential equation. General conclusions from the WKB-perturbation method can be drawn for absorbers, the layer thickness of which is either very small or very large in comparison to the wavelength. For "thin" layers, wave energy penetrates the whole thickness of the absorber. Suitable average values of the material constants are derived to describe the performance of the panel in this case. For "thick" layers only the initial part of the panel is energized. The asymptotic expressions contain only the material constants of this part. The results are interpreted physically. Numerical solutions of the reflection factor for highly refractive panels with exponentially varying material constants are reported.**

I. Introduction

THE PROBLEM of absorbing electromagnetic and acoustic waves is important for many applications in measuring techniques, for the construction of anechoic chambers, and for camouflaging targets in radar and sonar detection. Only plane waves, which propagate in a direction perpendicular to a plane absorbing surface, shall be considered here. The cases of electromagnetic and acoustic waves can be treated in complete analogy. Assuming normal incidence and isotropic media, the differential equations become identical in both cases. Various basic principles can be utilized in constructing absorbers. A good summary of these can be found in a paper by Meyer and Severin.[1]

One objective in absorber design is to achieve a low reflection factor over a frequency range as large as possible and simultaneously to keep the thickness l of the absorbing layer very small in comparison to the free field wavelength λ. This paper considers the principle of the gradual-transition absorber: A layer of lossy material covers a perfectly reflecting plane surface. By varying the material constants within the lossy panel, a good impedance match between the free propagation medium and the absorbing structure can be achieved. Such a gradual transition can be realized either by arranging a homogeneous lossy material in the form of wedges and pyramids or by using layers of varying material constants.

If the absolute amount r of the amplitude reflection factor for a gradual-transition absorber is plotted as a function of the ratio l/λ, the reflection decreases with some oscillations as l/λ increases. A satisfactory performance of absorbers can be specified by the requirement $r \leqq 10$ per cent. For well designed sound and microwave absorbers this condition can be realized in the range $l/\lambda \gtrsim 0.2$. For low frequencies a large layer thickness l would thus be required. One idea for the reduction of the l/λ-cutoff value is to apply lossy materials with a high index of refraction. Thus, the wavelength within the material can be reduced far below the free-field value. Artificially refractive media for microwaves and sound waves are well known.[2,3]

This paper derives the differential equations for the electromagnetic and acoustic inhomogeneous absorber. Some general conclusions for absorbers, which are either very thin or very thick in comparison to λ, are drawn. The performance of gradual-transition absorbers is then illustrated by several numerical solutions for highly refractive panels, in which the material constants vary according to exponential functions.

II. The Riccati-Differential Equation for the Gradual-Transition Absorber

A. Electromagnetic Waves

The theory of electromagnetic wave propagation in an inhomogeneous dielectric medium can be found in a paper by Barrar and Redheffer.[4] Consider a medium in which the material constants $\epsilon(x) = \epsilon'(x) - j\epsilon''(x)$ and $\mu(x) = \mu'(x) - j\mu''(x)$ depend on one coordinate x only. $\epsilon(x)$ and $\mu(x)$ are, respectively, the relative dielectric constant and permeability referred to the free-space values ϵ_0 and μ_0. A linearly polarized plane wave of time dependence exp $(j\omega t)$ is assumed to propagate in parallel to the x axis. Then Maxwellian equations read

$$\left.\begin{aligned} \frac{dH_z(x)}{dx} &= -j\omega\epsilon_0\epsilon(x)E_y(x) \\ \frac{dE_y(x)}{dx} &= -j\omega\mu_0\mu(x)H_z(x) \end{aligned}\right\}, \tag{1}$$

where

$E_y(x)$ = electric field strength
$H_z(x)$ = magnetic field strength.

* Received by the PGAP, April 14, 1960; revised manuscript received, June 16, 1960.
† Research Labs. Division, Bendix Corp., Southfield, Mich.
[1] E. Meyer and H. Severin, "Absorptionsanordnungen für elektromagnetische Zentimeterwellen und ihre akustischen Analogien," *Z. angew. Phys.*, vol. 8, pp. 105–114; March, 1956.
[2] W. E. Kock, "Metallic delay lenses," *Bell Sys. Tech. J.*, vol. 27, pp. 58–82; January, 1948.
[3] W. E. Kock and F. K. Harvey, "Refracting sound waves," *J. Acoust. Soc. Am.*, vol. 21, pp. 471–481; September, 1949.
[4] R. B. Barrar and R. M. Redheffer, "On nonuniform dielectric media," IRE Trans. on Antennas and Propagation, vol. AP-3, pp. 101–107; July, 1955.

An electric wave impedance $Z_e(x)$ can be defined for every position x within the layer:

$$Z_e(x) = -\frac{E_y(x)}{H_z(x)}. \tag{2}$$

The minus sign in this definition is necessary because of the choice of the coordinate system in Fig. 1. A differential equation satisfied by $Z_e(x)$ can be derived by means of (1):

$$\begin{aligned}\frac{dZ_e}{dx} &= -\frac{1}{H_z}\cdot\frac{dE_y}{dx} + \left(\frac{E_y}{H_z}\right)^2\cdot\frac{1}{E_y}\cdot\frac{dH_z}{dx} \\ &= j\omega\mu_0\mu(x) - j\omega\epsilon_0\epsilon(x)Z_e^2(x).\end{aligned} \tag{3}$$

The amplitude reflection factor $R_e(x)$ is defined

$$R_e(x) = \frac{Z_e(x) - Z_0}{Z_e(x) + Z_0}, \tag{4}$$

where $Z_0 = \sqrt{\mu_0/\epsilon_0} = 377\Omega$ = wave impedance of free space. Eq. (3) may be transformed into a Riccati-differential equation for $R_e(x)$:[5–7]

$$\frac{dR_e}{dx} = -j\frac{\pi}{\lambda_e}\left[\epsilon(x)(1+R_e)^2 - \mu(x)(1-R_e)^2\right] \tag{5}$$

where $\lambda_e = 2\pi/\omega\,(\epsilon_0\mu_0)^{-1/2}$ is the electric free space wavelength.

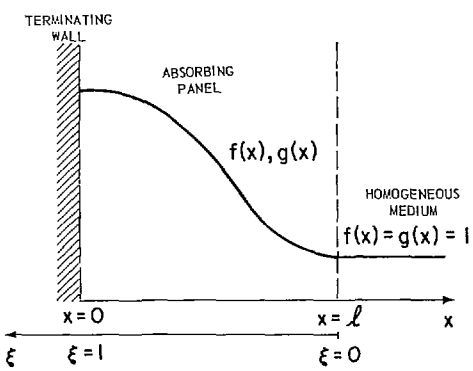

Fig. 1—Inhomogeneous absorbing panel of thickness l.

B. Acoustic Waves

The theory of acoustic wave propagation in an inhomogeneous medium can be found in a paper by Bergman.[8] The material constants $\kappa(x) = \kappa'(x) - j\kappa''(x)$ and $\rho(x) = \rho'(x) - j\rho''(x)$ of the acoustic medium are assumed to depend on one coordinate x only. $\kappa(x)$ and $\rho(x)$ are, respectively, the relative compressibility and density, referred to the values κ_0 and ρ_0 for the homogeneous medium in front of the absorber. A plane sound wave of time dependence $\exp(j\omega t)$ shall propagate in parallel to the x axis. Then the sound field equations for small amplitudes can be written

$$\left.\begin{aligned}\frac{dV(x)}{dx} &= -j\omega\kappa_0\kappa(x)P(x) \\ \frac{dP(x)}{dx} &= -j\omega\rho_0\rho(x)V(x)\end{aligned}\right\} \tag{6}$$

where $P(x)$ = sound pressure and $V(x)$ = particle velocity.

The acoustic wave impedance $Z_a(x)$ is defined

$$Z_a(x) = -\frac{P(x)}{V(x)}. \tag{7}$$

A differential equation for $Z_a(x)$ can be derived from (6):

$$\begin{aligned}\frac{dZ_a}{dx} &= -\frac{1}{V}\cdot\frac{dP}{dx} + \left(\frac{P}{V}\right)^2\cdot\frac{1}{P}\cdot\frac{dV}{dx} \\ &= j\omega\rho_0\rho(x) - j\omega\kappa_0\kappa(x)Z_a^2(x).\end{aligned} \tag{8}$$

The acoustic amplitude reflection factor $R_a(x)$ is given by

$$R_a(x) = \frac{Z_a(x) - Z}{Z_a(x) + Z}, \tag{9}$$

where $Z = \sqrt{\rho_0/\kappa_0}$ is the wave impedance of the homogeneous medium in front of the absorber. Eq. (8) may be transformed into a Riccati-differential equation for $R_a(x)$:

$$\frac{dR_a}{dx} = -j\frac{\pi}{\lambda_a}\left[\kappa(x)(1+R_a)^2 - \rho(x)(1-R_a)^2\right], \tag{10}$$

where $\lambda_a = 2\pi/\omega(\kappa_0\rho_0)^{-1/2}$ is the acoustic wavelength in the homogeneous medium in front of the absorber.

C. The Analogy

Since (5) and (10) are identical in form, the reflection factor R for the electromagnetic and acoustic cases can be evaluated by the same differential equation:

$$\frac{dR}{dx} = -j\frac{\pi}{\lambda}\left[g(x)(1+R)^2 - f(x)(1-R)^2\right], \tag{11}$$

where the analogy

$$f(x) = u(x) - jv(x) = \mu(x) \triangleq \rho(x) \tag{12}$$

$$g(x) = s(x) - jt(x) = \epsilon(x) \triangleq \kappa(x) \tag{13}$$

between electric and acoustic quantities is used.

According to (4) and (9) a boundary condition $R = +1$ corresponds to a "magnetic" wall (surface of zero magnetic field strength) in the electromagnetic case and to a rigid wall in the acoustic case. The condition $R = -1$ requires an "electric" wall (metal plate) or a pressure

[5] R. M. Redheffer, "Reflection and transmission equivalences of dielectric media," Proc. IRE, vol. 39, p. 503; May, 1951.
[6] R. M. Redheffer, "Novel uses of functional equations," *J. Rat. Mech. Anal.*, vol. 3, pp. 271–279; March, 1954.
[7] R. M. Redheffer, "Limit-periodic dielectric media," *J. Appl. Phys.*, vol. 27, pp. 1136–1140; October, 1956.
[8] P. G. Bergman, "The wave equation in a medium with a variable index of refraction," *J. Acoust. Soc. Am.*, vol. 17, pp. 329–333; April, 1946.

release surface in the two cases, respectively. Interchanging $f(x)$ and $g(x)$ in (11) is equivalent to changing the sign of $R(x)$. According to (4) and (9) this corresponds to replacing impedance by admittance and vice versa. This is the well-known principle of duality.

III. Some General Properties of the Reflection Factor for the Gradual-Transition Absorber

A. Interpretation of the Reflection Factor for an Inhomogenous Medium

The geometry of the problem under consideration is shown in Fig. 1. An absorbing panel is terminated at $x=0$ by a totally reflecting wall. At the front surface $x=l$ the material constants shall be the same as for the homogeneous propagation medium, $f(x)=g(x)=1$ for $x\geq l$. The gradual transition of material constants is represented schematically by the functions $f(x)$ and $g(x)$. A solution $R(x)$ can be computed from (11) with the proper initial condition at $x=0$. The point $R(l)$ is the reflection factor of the total layer. A physical interpretation of the solution $R(x)$ is possible also for a point $x_0\neq l$. The definition of $R(x)$ in (4) is due to Redheffer.[5] The Redheffer-reflection factor $R(x_0)$ represents the reflection from an inhomogeneous panel, in which the region $x_0\leq x\leq l$ has been replaced by a homogeneous medium of material constants $f(x)=g(x)=1$ (Fig. 2).

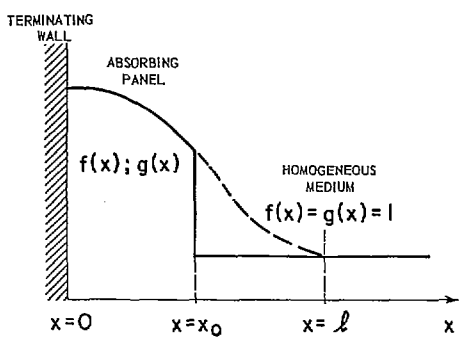

Fig. 2—Interpretation of the Redheffer reflection factor at $x=x_0$.

A different approach to the problem of wave propagation in an inhomogeneous medium may be found by defining the reflection factor $R_s(x)$:

$$R_s(x) = \frac{Z_e(x) - \sqrt{\mu(x)/\epsilon(x)}}{Z_e(x) + \sqrt{\mu(x)/\epsilon(x)}}, \tag{14}$$

instead of using (4). Kay[9] associates this approach with the name of Schelkunoff (see additional references in his paper[9]) and compares several aspects of the "Redheffer" and "Schelkunoff" methods. The definition in (14) leads to a different Riccati equation for $R_s(x)$, requiring $f(x)$ and $g(x)$ to be differentiable. A solution $R_s(x)$ at $x=x_0\neq l$ corresponds to the reflection from an inhomogeneous layer, in which the whole region $x\geq x_0$ has been replaced by a homogeneous medium of material constants $f(x_0)$ and $g(x_0)$ (Fig. 3). Since in general $f(x_0)$ and $g(x_0)\neq 1$, the intermediate points $R_s(x_0)$ according to the Schelkunoff method do not represent physically interesting solutions for the absorber problem. On the other hand, the intermediate points of the Redheffer solution (Fig. 2) may give useful information on the effect of cutting away part of the panel (reduction of layer thickness, effect of an initial step). For the point $x=l$ the results of both methods are identical, if layers with no initial step are considered. An example of the Schelkunoff method for calculating the reflection factor of gradual-transition sound absorbers can be found in a paper by Miller.[10] We prefer to use the Redheffer method in this paper.

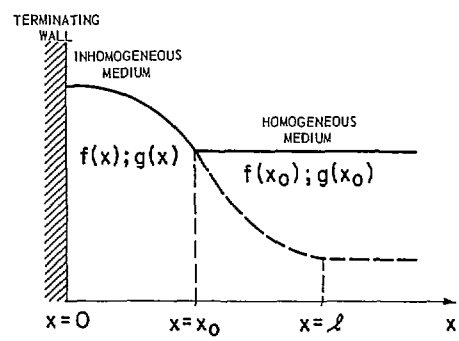

Fig. 3—Interpretation of the Schelkunoff reflection factor at $x=x_0$.

B. Behavior of Panels, Thin Compared to Wavelength

Integration of the Riccati equation (11) normally leads to nonelementary functions and has to be accomplished numerically; such results are reported in Section IV. Some general conclusions can be drawn, however, for the limiting cases of a layer thickness l which is either very small or very large in comparison to the wavelength λ.

1) Taylor-Series Solution of the Riccati Equation: For the case $l/\lambda \ll 1$ the quantity $r(x)=|R(x)|$ may be calculated from (11) in the form of a Taylor series, starting at the point $x=0$:

$$r(x) = \sum_{\nu=0}^{\infty} \left(\frac{d^{(\nu)}r}{dx^{\nu}}\right)_0 \frac{x^{\nu}}{\nu!}. \tag{15}$$

A similar method has been applied by Sampson.[11] Results shall be given here only for two simple cases (Table I). These can be characterized physically by the facts: Case 1 shows *high* energy dissipation near the terminating surface $x=0$. In Case 2 a *low* energy dissipa-

[9] A. F. Kay, "Reflection of a Plane Wave by a Stratified Medium," McMillan Lab., Inc., Ipswich, Mass. Tech. Rept., Contract AF18(600)-1044; November 22, 1954.

[10] N. B. Miller, "Reflections from gradual transition sound absorbers," *J. Acoust. Soc. Am.*, vol. 30, pp. 967–973; October, 1958.

[11] J. H. Sampson, "Some Absorbing Panels with Variable Dielectric Composition," McMillan Lab., Inc., Ipswich, Mass., Tech. Rept., Contract AF18(600)-1044; December 20, 1954.

TABLE I

Case 1: High Energy Dissipation Near $x=0$	Case 2: Low Energy Dissipation Near $x=0$
Electromagnetic Waves	
a) Electric losses—Magnetic wall b) Magnetic losses—Electric wall	a) Electric losses—Electric wall b) Magnetic losses—Magnetic wall
Acoustic Waves	
a) Compressibility losses—Rigid wall b) Density (friction) losses—Pressure release wall	a) Compressibility losses—Pressure release wall b) Density (friction) losses—Rigid wall

tion near the terminating surface $x=0$ prevails. The energy N dissipated per unit volume is proportional to:

for electromagnetic waves:

$$N_e \sim \epsilon'' \cdot E^2 + \mu'' \cdot H^2$$

for acoustic waves:

$$N_a \sim \kappa'' \cdot P^2 + \rho'' \cdot V^2.$$

In the following cases we assume that only one type of loss mechanism is present, putting either $f(x)$ or $g(x)=1$ in (11). The possible "simple" cases are summarized in Table I.

The cases that can be realized most easily in absorber design are Case 2a) for microwaves, Case 1a) for waterborne sound, and Case 2b) for airborne sound. The Taylor-series expansion of (15) shall be given for Cases 1a) and 2a) as examples: $t(x)=\epsilon''(x)$,

Case 1a):

$$r(x) \simeq 1 - \frac{4\pi}{\lambda}\epsilon''(0)x + \left[\frac{8\pi^2}{\lambda^2}\epsilon''^2(0) - \frac{2\pi}{\lambda}\left(\frac{d\epsilon''}{dx}\right)_0\right]\cdot x^2 + \cdots \quad (16)$$

Case 2a):

$$r(x) \simeq 1 - \frac{16\pi^3}{3\lambda^3}\epsilon''(0)x^3 - \frac{4\pi^3}{\lambda^3}\left(\frac{d\epsilon''}{dx}\right)_0 \cdot x^4 + \cdots. \quad (17)$$

These curves are shown in Fig. 4. For the case of high energy dissipation a sharp drop of $r(x)$ near $x=0$ can be observed. In the case of low energy dissipation the curve $r(x)$ starts from the point, $r=1$, with a horizontal slope, the deviation being given by a third-order term.

It should be emphasized that the convergence of the series (15) is very poor. Moreover, this approach is not very satisfactory for a physical interpretation, since only functional values and derivatives at $x=0$ are specified. For very "thin" layers energy is penetrating the full thickness l of the absorber. Therefore, it can be expected physically that certain average values of the material constants $f(x)$ and $g(x)$ in the form of integrals $\int_0^l f(x)\cdot w_1(x)dx$ and $\int_0^l g(x)\cdot w_2(x)dx$ are more appropriate for the description of very "thin" layers. These relations will now be derived.

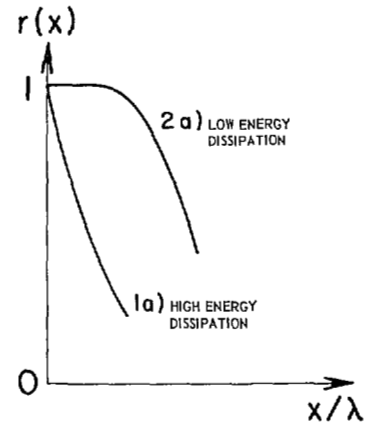

Fig. 4—Initial behavior of the reflection factor $r(x)$ for "thin" absorbers: $x/\lambda \ll 1$.

2) WKB Solution of the Wave Equation: The WKB perturbation method for obtaining approximate solutions of the inhomogeneous wave equation has proved useful in many problems of quantum mechanics and wave propagation.[12] We follow a treatise by Zharkovskii and Todes,[13] but we consider a more general case. Similar approximation methods can be found in a paper by Pipes.[14]

The wave equation for the electric field strength $E(\xi)$ can be derived from (1), where the coordinate transformation $\xi = 1 - x/l$ has been used (see Fig. 1):

$$\frac{d^2E}{d\xi^2} - \frac{d(\ln\mu(\xi))}{d\xi}\cdot\frac{dE}{d\xi} + (kl)^2\epsilon(\xi)\mu(\xi)E(\xi) = 0, \quad (18)$$

[12] See, *e.g.*, references in C. O. Hines, "Reflection of waves from varying media," *Quart. J. Appl. Math.*, vol. 11, pp. 9–31; April, 1953.

[13] A. G. Zharkovskii and O. M. Todes, "Reflection of waves from an isotropic inhomogeneous layer," *Soviet Phys. JETP*, vol. 4, pp. 701–703; June, 1957.

[14] L. A. Pipes, "Computation of the impedances of nonuniform lines by a direct method," *Trans. AIEE*, vol. 75, pp. 551–554; November, 1956.

where $kl = 2\pi l/\lambda$. A solution of this equation is sought in the form:

$$E(\xi) = E^{+}\cdot\exp\left(jkl\cdot\int_1^{\xi} f_s(\xi)d\xi\right) + E^{-}\cdot\exp\left(-jkl\cdot\int_1^{\xi} F_s(\xi)d\xi\right). \quad (19)$$

The functions $f_s(\xi)$ and $F_s(\xi)$ satisfy the following first-order differential equations:

$$-jkl[\epsilon\mu - f_s^2] + \left[\frac{df_s}{d\xi} - \frac{d(\ln\mu)}{d\xi} f_s\right] = 0 \quad (20)$$

and

$$+jkl[\epsilon\mu - F_s^2] + \left[\frac{dF_s}{d\xi} - \frac{d(\ln\mu)}{d\xi} F_s\right] = 0. \quad (21)$$

For the case of very thin layers $kl \ll 1$ we use asymptotic expansions of the form:

$$f_s(\xi) = \sum_{m=0}^{\infty} k^m f_{s,m}(\xi) \quad (22)$$

and

$$F_s(\xi) = \sum_{m=0}^{\infty} k^m F_{s,m}(\xi). \quad (23)$$

Eqs. (20) and (21) are solved by a perturbation method. An approximate solution $E(\xi)$ satisfying the short-circuit boundary condition at $\xi = 1$ can thus be derived:

$$E(\xi) = A\cdot\exp\left[-(kl)^3 \cdot\int_1^{\xi}\mu(\xi')\int_1^{\xi'}(\epsilon-\mu)d\xi''d\xi'\right]\sin\phi(\xi), \quad (24)$$

where

$$\phi(\xi) = kl\cdot\int_1^{\xi}\mu(\xi')d\xi' + 2(kl)^3 \cdot\int_1^{\xi}\mu(\xi')\int_1^{\xi'}\mu(\xi'')\int_1^{\xi''}(\epsilon-\mu)d\xi'''d\xi''d\xi'.$$

This expansion is correct including terms of order $(kl)^3$. By application of Maxwell's equations (1) the normalized input admittance for the front surface $\xi = 0$ of the layer may be derived:

$$\frac{Y_i}{Y_o} = jkl\cdot\int_0^1(\epsilon-\mu)d\xi' - j[1 + 2(kl)^2 \cdot\int_0^1\mu(\xi')\int_{\xi'}^1(\epsilon-\mu)d\xi''d\xi']\operatorname{cotan}\phi(\xi). \quad (25)$$

After some mathematical manipulations, including removal of multiple integrations, (25) can be rewritten for the normalized input impedance and may be interpreted physically for simple cases.

Assuming $\mu(\xi) \equiv 1$, the result, including terms of order $(kl)^3$, reads

$$\frac{Z_i}{Z_o} = jkl + j\frac{(kl)^3}{3}\int_0^1\epsilon(\xi)w_1(\xi)d\xi, \quad (26)$$

where the weighting function

$$w_1(\xi) = 3(1-\xi)^2; \qquad \int_0^1 w_1(\xi)d\xi = 1 \quad (27)$$

has been introduced. If this result is written in the form

$$\frac{Z_i}{Z_o} = jkl + j\cdot\frac{(kl)^3}{3}\cdot\bar{\epsilon} = jkl + j\cdot\frac{(kl)^3}{3}\cdot\overline{\epsilon'} + \frac{(kl)^3}{3}\cdot\overline{\epsilon''}, \quad (28)$$

it is equivalent to the input impedance of a homogeneous layer with average dielectric constant.

$$\bar{\epsilon} = \int_0^1\epsilon(\xi)w_1(\xi)d\xi. \quad (29)$$

In the case $\epsilon(\xi) \equiv 1$, the expansion of the normalized input impedance may be written.

$$\frac{Z_i}{Z_o} = jkl\int_0^1\mu(\xi)d\xi + j(kl)^3\cdot 2\int_0^1\xi\mu(\xi)\int_{\xi}^1\mu(\xi')d\xi'd\xi. \quad (30)$$

In order to show the physical significance of this result more clearly, we consider a layer in which the permeability $\mu(\xi)$ differs by only a small amount $\nu(\xi)$ from the homogeneous value μ: $\mu(\xi) = \mu + \nu(\xi)$. For this case we can rewrite (30) in the form

$$\frac{Z_i}{Z_0} = jkl\cdot\int_0^1\mu(\xi)w_2(\xi)d\xi + j\frac{(kl)^3}{3}\left[\left(\int_0^1\mu(\xi)w_3(\xi)d\xi\right)^2 + \Delta\right], \quad (31)$$

where the error Δ

$$\Delta = 6\int_0^1\xi\nu(\xi)\int_{\xi}^1\nu(\xi')d\xi'd\xi - \left[\int_0^1\nu(\xi)w_3(\xi)d\xi\right]^2 \quad (32)$$

is a second-order term in $\nu(\xi)$ and can be neglected, whenever $|\nu(\xi)| \ll \mu$. Thus, the almost homogeneous layer can be represented within a good approximation by means of two weighting functions:

$$w_2(\xi) \equiv 1 \quad (33)$$

$$w_3(\xi) = 3\xi - \frac{3}{2}\xi^2; \qquad \int_0^1 w_3(\xi)d\xi = 1 \quad (34)$$

which are different for the two degrees of expansion in (kl).

These analogies with the homogeneous case suggest the definition of two average values of the permeability:

$$\bar{\mu} = \int_0^1 \mu(\xi) d\xi \tag{35}$$

$$(\tilde{\mu})^2 = 6 \int_0^1 \xi\mu(\xi) \int_\xi^1 \mu(\xi') d\xi' d\xi. \tag{36}$$

Using these values, (30) may be rewritten

$$\frac{Z_i}{Z_o} = jkl\bar{\mu} + j \cdot \frac{(kl)^3}{3} \cdot (\tilde{\mu})^2 \simeq jkl \cdot \overline{\mu'} + kl \cdot \overline{\mu''} + \cdots \tag{37}$$

This is a well-known result for the homogeneous case, where $\bar{\mu} = \tilde{\mu} = \mu$.

The weighting functions $w_1(\xi)$ through $w_3(\xi)$ for a short-circuit termination at $\xi = 1$ are plotted in Fig. 5. A physical interpretation suggests that $w_1(\xi)$ has to be zero near $\xi = 1$, because in a region of low electric field strength a dielectric constant of the material cannot be effective. From (27) it could be concluded that a variation of dielectric constant

$$\epsilon(\xi) \sim (1 - \xi)^{-2} \tag{38}$$

would result in a constant value of the weighted dielectric constant $\epsilon(\xi) \cdot w_1(\xi)$ throughout the layer and should have favorable applications in absorber design. Such a function (38) was considered by Jacobs.[15] This author arrives at (38) by attempting to find a function $\epsilon(\xi)$, for which the fractional change $1/\epsilon \cdot d\epsilon/d\xi$ referred to the "local" wavelength $\lambda(\xi) = \lambda/\sqrt{\epsilon(\xi)}$ is the same small constant a for all positions ξ within the layer:

$$\frac{1}{2\pi\epsilon(\xi)} \cdot \frac{d\epsilon}{\dfrac{d\xi}{\lambda(\xi)}} = \frac{\lambda}{2\pi} \cdot \frac{1}{\epsilon^{3/2}} \cdot \frac{d\epsilon}{d\xi} = a \ll 1.$$

This statement may be similar to our interpretation of (38). Because of the singularity of (38) at $\xi = 1$ we have to be cautious, however, in drawing too many conclusions from perturbation theory.

From a similar physical reasoning the weighting function $w_2(\xi)$ should be unity near the short circuit $\xi = 1$, since in a region of maximum magnetic field strength the permeability can be fully effective. The higher order weighting function $w_3(\xi)$ should decrease with the distance from the terminating wall, since the magnetic field strength decreases. The functions $w_1(\xi)$ and $w_3(\xi)$ should thus have an opposite trend.

Assuming frequency independent material constants ϵ and μ, the impedance curves corresponding to (28) and (37) are shown schematically in Fig. 6. For the case of electric losses (curve 1), the deviation from the imaginary axis is given by a third-order term in ω. In the case of magnetic losses (curve 2), the impedance curve starts at an angle ψ off the imaginary axis, where $\tan \psi = \overline{\mu''}/\overline{\mu'}$.

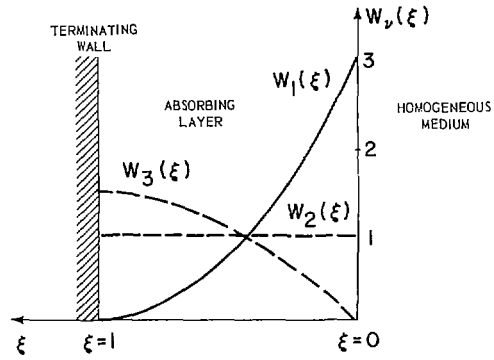

Fig. 5—Weighting functions $w_\nu(\xi)$ for "thin" absorbers:

$$w_1(\xi) = 3(1 - \xi)^2,$$
$$w_2(\xi) \equiv 1,$$
$$w_3(\xi) = 3\xi - \frac{3}{2}\xi^2$$
$$\int_0^1 w_\nu(\xi) d\xi = 1.$$

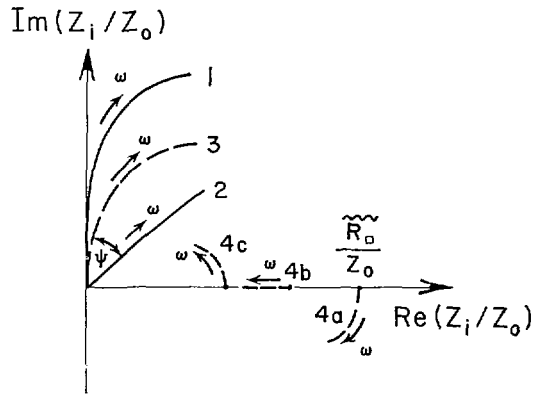

Fig. 6—Impedance curves for "thin" absorbers.

(a) $\tilde{Y}_\square < Y_c$, (b) $\tilde{Y}_\square = Y_c$, (c) $\tilde{Y}_\square > Y_c$.

Curve 1: electric losses, short-circuit termination.
Curve 2: magnetic losses, short-circuit termination; $\tan \psi = \overline{\mu''}/\overline{\mu'}$.
Curve 3: conductivity losses, short-circuit termination.
Curve 4: conductivity losses, open-circuit termination.
$Y_\square$ = averaged value of the "area-conductance."
Y_c = critical value of the "area-conductance."

The reflection factors corresponding to (28) and (37) are

$$|R| \simeq 1 - \frac{16\pi^3}{3\lambda^3} l^3 \overline{\epsilon''} + \cdots \text{ for electric losses} \tag{39}$$

and

$$|R| \simeq 1 - \frac{4\pi}{\lambda} \cdot l\overline{\mu''} + \cdots \text{ for magnetic losses.} \tag{40}$$

These functions are shown in Fig. 7, curves 1 and 2. A comparison with the initial parts of (16) and (17) shows that the averaged values of ϵ'' and μ'' have been substituted for the initial values at $\xi = 1$. [Instead of (16) the dual case has to be considered.]

[15] I. Jacobs, "The nonuniform transmission line as a broadband termination," *Bell Sys. Tech. J.*, vol. 37, pp. 913–924; July, 1958.

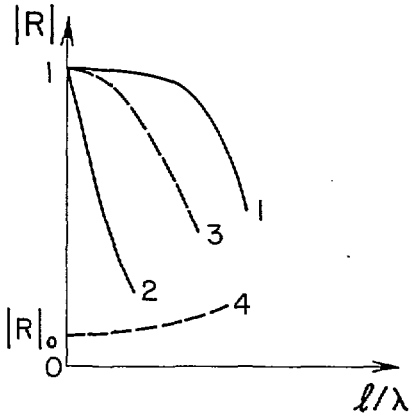

Fig. 7—Initial behavior of the reflection factor $|R|$ for "thin" absorbers: $l/\lambda \ll 1$.
Curve 1: electric losses, short-circuit termination.
Curve 2: magnetic losses, short-circuit termination.
Curve 3: conductivity losses, short-circuit termination.
Curve 4: conductivity losses, open-circuit termination.

$$|R|_0 = \left|\frac{R_\square - Z_0}{R_\square + Z_0}\right|.$$

A different result is obtained if frequency dependent losses are taken into account. A loss mechanism, in which the loss factor is proportional to ω^{-1}, has special interest for very thin panels at low frequencies. Examples of such loss mechanisms are: 1) ohmic conductivity σ in the case of electromagnetic waves and 2) viscous friction in the case of acoustic waves (porous absorbers). Only the first case shall be considered here.

Substituting the expression for $\overline{\epsilon''} = \bar{\sigma}/\omega\epsilon_0$ into (28) gives the following result for the short-circuit case:

$$\frac{Z_i}{Z_o} = j\Omega + \frac{1}{3}\cdot\Omega^2\cdot\frac{Z_o}{\overline{R}_\square} + j\cdot\frac{\Omega^3}{3}\cdot\bar{\epsilon}' + \cdots. \tag{41}$$

Here the normalized frequency $\Omega = (\omega/c)l$ and the averaged "area-resistance" $\overline{R}_\square = 1/\bar{\sigma}l$ of the layer have been introduced, where $\bar{\sigma} = \int_0^1 \sigma(\xi)\cdot w_1(\xi)d\xi$ is the averaged conductivity. The reflection factor corresponding to (41) reads

$$|R| \simeq 1 - \frac{8\pi^2}{3\lambda^2}\cdot l^2\cdot\frac{Z_o}{\overline{R}_\square} + \cdots. \tag{42}$$

These relations are shown graphically as curve 3 in both Fig. 6 and Fig. 7. The deviation of the impedance curve 3 (Fig. 6) from the imaginary axis is given by a second-order term in ω and thus is much more effective than in the case of curve 1. Fig. 7 shows that the reflection factor for curve 3 drops much faster with increasing l/λ as compared to curve 1. The low-frequency properties of a "thin" conductive layer with short-circuit termination can be described qualitatively by the equivalent circuit of Fig. 8.[16]

The case of a conductive layer with open-circuit termination at $\xi = 1$ gives considerably different results. If $\epsilon(\xi)$ is substituted instead of $\mu(\xi)$ and the normalized

[16] *Ibid.*, p. 916.

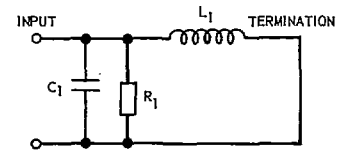

Fig. 8—Approximate equivalent circuit for the "thin" conductive layer with short-circuit termination.

input admittance Y_i/Y_o is written instead of Z_i/Z_o the following result can be obtained directly from (37):

$$\frac{Y_i}{Y_o} = jkl\tilde{\epsilon} + j\cdot\frac{(kl)^3}{3}\cdot(\tilde{\epsilon})^2. \tag{43}$$

By inserting the value $\epsilon = \epsilon' - j(\sigma/\omega\epsilon_0)$ the expansion including linear terms in frequency can be written.

$$\frac{Y_i}{Y_0} = \frac{\tilde{Y}_\square}{Y_0} - j\Omega\left[\frac{1}{3}\cdot\left(\frac{\tilde{Y}_\square}{Y_o}\right)^2 - \tilde{\epsilon}'\right], \tag{44}$$

where $\Omega = (\omega/c)l$ is the normalized frequency and $\tilde{\epsilon}' = \int_0^1 \epsilon'(\xi)d\xi$. Two averaged values for the "area-conductance" of the layer have been introduced:

$$\tilde{Y}_\square = \tilde{\sigma}l, \quad \text{where} \quad \tilde{\sigma} = \int_0^1 \sigma(\xi)d\xi \tag{45}$$

$$\tilde{Y}_\square = \tilde{\sigma}l, \quad \text{where} \quad (\tilde{\sigma})^2 = 6\int_0^1 \xi\sigma(\xi)\int_\xi^1 \sigma(\xi')d\xi'd\xi. \tag{46}$$

The normalized input impedance Z_i/Z_o corresponding to (44) is plotted as curves 4a through 4c in Fig. 6. All these curves start with a finite real value of the input impedance $Z_i = \tilde{R}_\square = 1/\tilde{Y}_\square$. The reactive behavior depends on the value of the average area-conductance $\tilde{Y}_\square$ with respect to a critical value

$$Y_c = Y_o\cdot\sqrt{3\tilde{\epsilon}'}. \tag{47}$$

Low conductive layers with $\tilde{Y}_\square > Y_c$ show a capacitive component; highly conductive layers with $\tilde{Y} \leq Y_c$ are inductive. In the case $\tilde{Y}_\square = Y_c$, the first-order reactive component is zero. From higher-order approximations the frequency dependence of curves 4a through 4c in Fig. 6 can be derived. The equivalent circuit of Fig. 9 qualitatively shows the same behavior if the resistance R_2 is varied with respect to the wave impedance $\sqrt{L_2/C_2}$. The reflection factor corresponding to (44) starts with a finite value

$$|R|_0 = \left|\frac{\tilde{R}_\square - Z_0}{\tilde{R}_\square + Z_0}\right|$$

These facts are familiar from the theory of the Salisbury screen, for which the area-resistance is chosen to be $R_\square = 377\ \Omega$ in order to match the absorber. The open-circuit termination in the case of electromagnetic waves can be realized in a resonance condition by placing a resistive foil at a distance of $\lambda/4$ in front of a metal plate. A "magnetic" wall can only be approximated

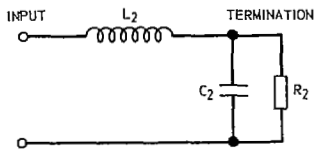

Fig. 9—Approximate equivalent circuit for the "thin" conductive layer with open-circuit termination.

roughly over a limited frequency band below the microwave range by using media with $|\mu| \gg |\epsilon|$ (for instance, ferrites).

The analogous acoustic case would be a porous absorber in water near a pressure release surface. Such porous materials (for instance fiberglass) are very effective as absorbers for airborne sound. However, the achievable friction losses with porous frameworks or similar structures for waterborne sound are much more limited.[17,18] The reason for this is partly that a motion of the absorbing structure cannot be avoided at low frequencies, thus the achievable friction is limited. Although the acoustic analog of a "magnetic" wall can be realized easily, for the reasons mentioned, the required layer thickness of the absorber would be rather large. Therefore the analysis for the "thin" layer cannot be applied in this case.

C. Behavior of Panels, Thick Compared to Wavelength

Section III-B dealt with the theory of the "thin" layer. The analysis and interpretation have to be rather detailed, because energy penetrates the full layer thickness l. If the other limiting case of panels, thick compared to wavelength, is considered, we should expect physically a simpler situation. In this case only the initial part of the layer near the front surface $\xi=0$ is energized. The multiple reflections from the terminating wall $\xi=1$ become more and more insignificant as the frequency increases.

The analysis of the "thick" layer starts in a way that is analogous to the derivations in Section III-B, 2).[13] A solution of the wave equation (18) is sought in the form of (19), with (20) and (21) being the same. Instead of the asymptotic expansions (22) and (23) we use

$$f_s(\xi) = \sum_{m=0}^{\infty} \left(\frac{1}{k}\right)^m f_{s,m}(\xi) \tag{48}$$

$$F_s(\xi) = \sum_{m=0}^{\infty} \left(\frac{1}{k}\right)^m F_{s,m}(\xi), \tag{49}$$

for the case $kl \gg 1$. The differential equations (20) and (21) are solved by a perturbation method. A solution $E(\xi)$ satisfying the short-circuit boundary condition at the terminating wall $\xi=1$ can thus be derived:

$$E(\xi) = A \exp\left[\frac{1}{2}\int_1^{\xi} \frac{d}{d\xi}\left(\ln \sqrt{\frac{\mu}{\epsilon}}\right) d\xi\right] \sin\left(kl \int_1^{\xi} \sqrt{\epsilon\mu}\, d\xi\right). \tag{50}$$

The normalized input admittance for the front surface $\xi=0$ can be computed by means of Maxwell's equations (1):

$$\frac{Y_i}{Y_o} = \frac{-j}{4kl\mu(0)}\left[\frac{d \ln \epsilon}{d\xi} - \frac{d \ln \mu}{d\xi}\right]_{\xi=0} - j\sqrt{\frac{\epsilon(0)}{\mu(0)}} \operatorname{cotan}\left(kl \int_0^1 \sqrt{\epsilon\mu}\, d\xi\right). \tag{51}$$

Considering a layer without an initial discontinuity, $\epsilon=\mu=1$ for $\xi=0$, (51) can be simplified:

$$\left.\begin{aligned} \frac{Y_i}{Y_o} &= \frac{-j}{4kl}\left[\left(\frac{d\epsilon}{d\xi}\right)_0 - \left(\frac{d\mu}{d\xi}\right)_0\right] - j\cdot\operatorname{cotan}\left(kl\cdot\int_0^1 \sqrt{\epsilon\mu}\, d\xi\right) \\ &= \frac{j(\dot{u} - \dot{s})_0 + (\dot{v} - \dot{t})_0}{4kl} - j\cdot\operatorname{cotan}\left(kl\cdot\int_0^1 \sqrt{\epsilon\mu}\, d\xi\right) \end{aligned}\right\}, \tag{52}$$

where

$$(\dot{u})_0 = \left(\frac{du}{d\xi}\right)_{\xi=0}, \text{ etc.}$$

The real and imaginary parts of $\mu(\xi)$ and $\epsilon(\xi)$ have been substituted from (12) and (13).

Consider the case of frequency independent material constants $\epsilon(\xi)$ and $\mu(\xi)$ first. Then the impedance curve corresponding to the first term in (52) runs to zero along a straight line in the complex plane as $\omega \to \infty$. The second term in (52) represents the short-circuit input admittance of a transmission line with an averaged refraction index:

$$\bar{n} = \int_0^1 \sqrt{\epsilon(\xi)\mu(\xi)}\, d\xi \tag{53}$$

According to our assumptions, no initial discontinuity of wave impedance for this equivalent transmission line is present at $\xi=0$. From transmission line theory it is well known that the corresponding impedance plot is a spiral in the complex plane, approaching the point $Y_i/Y_o = +1$ in a clockwise sense as $\omega \to \infty$. In (52) both the real and imaginary part of the argument for the cotan function increase proportional to frequency. Therefore, the distance between any point of the spiral $Y_i/Y_o = -j \operatorname{cotan}(kl \cdot \int_0^1 \sqrt{\epsilon\mu}\, d\xi)$ and the limiting point $Y_i/Y_o = +1$ vanishes according to an exponential function of general form exp $(-\text{const } l/\lambda)$. Since the first

[17] E. Meyer and K. Tamm, "Breitbandabsorber für Flüssigkeitsschall," *Acustica*, vol. 2, Beiheft 2, pp. AB 91–AB 104; 1952.

[18] K. Tamm, "Broad-band absorbers for water-borne sound," in E. G. Richardson, "Technical Aspects of Sound," Elsevier Publishing Co., New York, N. Y., vol. 2, ch. 6, pp. 240–286; 1957.

term in (52) only vanishes like an inverse power in (l/λ), this is the significant part for the calculation of the reflection factor $|R|$ in the limiting case $\omega \to \infty$. Thus the following result can be obtained:

$$|R|_{l/\lambda \to \infty} = \frac{\sqrt{(\dot{u} - \dot{s})_0^2 + (\dot{v} - \dot{t})_0^2}}{\frac{16\pi}{\lambda} l}. \tag{54}$$

The reflection factor vanishes like $(l/\lambda)^{-1}$ for $l/\lambda \to \infty$. The only quantities of the layer which appear in this equation are the first order derivatives of the material constants at the front surface $\xi = 0$. Reflections from the terminating wall can be neglected completely, since no energy enters this part of the absorber. By application of Schwarz's inequality, Kay[9] has shown, generally, that the Schelkunoff-reflection factor R_s (14) cannot vanish as a weaker power than $\lambda^{1/2}$ for the limit $\lambda \to 0$.

Eq. (54) breaks down for the case

$$\epsilon(\xi) \equiv \mu(\xi), \tag{55}$$

because then the first term in (52) vanishes. However, in this case it is easy to derive an exact solution for R from (11):

$$|R| = \exp\left(-\frac{4\pi}{\lambda} l \int_0^1 v(\xi) d\xi\right). \tag{56}$$

Thus, an exponential decay of $|R|$ for all values l/λ should be expected.

Eq. (52) shows that, in the general case, both effects are present simultaneously. The qualitative course of $|R|$ with increasing l/λ can thus be described as follows. The reflection factor $|R|$ shows damped oscillations around a decreasing average value. The decrease of the average level is determined by the combination of an inverse power term and an exponential term in l/λ. This also can be seen by plotting some of the numerical curves of Section IV on a double or semi-logarithmic scale. In neither of the two cases straight lines are obtained. Moreover, (52) shows that by increasing one type of material losses the oscillatory term can be damped out faster with increasing l/λ. However, at the same time the average level represented by the inverse power term is raised. Therefore, a compromise in choosing material losses is necessary according to the selected performance criterion for the absorber. The numerical solutions in Section IV shall illustrate these statements.

In the case of ohmic conductivity losses (54) is not valid either. This can be seen from (52). Assuming $\mu(\xi) = 1$, the argument of the cotan-function can be approximated for very high frequencies:

$$kl \cdot \int_0^1 \sqrt{\epsilon'(\xi) - j \cdot \frac{\sigma(\xi)}{\omega \epsilon_0}}\, d\xi \simeq \frac{\omega}{c} l \cdot \int_0^1 \sqrt{\epsilon'(\xi)}\, d\xi - j \frac{l}{2c\epsilon_0} \int_0^1 \frac{\sigma(\xi)}{\sqrt{\epsilon'(\xi)}}\, d\xi. \tag{57}$$

The impedance values of the function $-j \cdot \text{cotan}\,(kl \int_0^1 \sqrt{\epsilon}\, d\xi)$ are located on a closed limit-curve $(\omega \to \infty)$ around the point $+1$, which is determined by the finite imaginary part in (57). Since the real part in (57) increases with ω, rotations along this limiting curve continue with increasing l/λ. The reflection factor, according to the cotan-term in (52), does not approach zero, but shows fluctuations between two finite values which are determined by the distance from the limiting-curve to the point $+1$. For these considerations see also the papers of Lenz and Zinke.[19,20]

IV. Numerical Solutions of $|R|$ for Absorbers with Exponentially Varying Material Constants

In this section some numerical solutions for the absolute amount r of the reflection factor of gradual-transition absorbers shall be reported. These solutions have been calculated from the differential equation (11) by means of a Bendix analog computer. Some check solutions on an IBM 650 digital computer have been computed also. The accuracy of the calculations is estimated to be $\Delta r = \pm 1$ per cent.

Lenz[20] carried out many analog measurements on electrical models of gradual-transition absorbers, in order to determine optimum functions for the variation of the material constants within the layer. In these measurements ohmic conductivity losses were studied, the real part of the dielectric constant being unity. A short circuit termination of the layer was assumed. In the investigations of Lenz, layers with exponentially varying conductivity losses show a favorable result. The condition $r < 10$ per cent can be satisfied for all $l/\lambda \geq 0.35$. Layers with three sections of piece-wise constant conductivity even show a slightly better result: $r \leq 10$ per cent for all $l/\lambda \geq 0.33$. Numerical calculations of Sampson[11] on some highly refractive dielectric panels also show some advantages for exponentially varying material constants.

For these reasons we choose exponential functions to describe the variations of material constants in the numerical solutions. For the first part of the calculations [Figs. 10 through 18(b), pp. 618–619] we consider "simple" cases according to Table I, for which either $f(x) = 1$ or $g(x) = 1$ in (11). As an example the functions $s(x)$ and $t(x)$ and the boundary conditions for $R(x)$ at $x = 0$ are specified in Figs. 10 through 18(b). The physical interpretation of the results for either electromagnetic or acoustic waves can be accomplished easily by means of Table I and the analogy given in Section II-C, including the principle of duality. We consider the general form of

[19] K. L. Lenz and O. Zinke, "Die Absorption elektromagnetischer Wellen in Absorbern und Leitungen mit abschnittweise homogenem Leitwertsbelag," *Z. angew. Phys.*, vol. 9, pp. 481–489; October, 1957.

[20] K. L. Lenz, "Leitungen mit ortsabhängiger Dämfung zur reflexionsarmen Absorption elektromagnetischer Wellen," *Z. angew. Phys.*, vol. 10, pp. 17–25; January, 1958.

functions $g(x)=s(x)-j\cdot t(x)$:

$$s(x) = a^{(1-x/l)} \tag{58}$$

$$t(x) = b^{(1-x/l)} - d. \tag{59}$$

A more special form of equation (59) is also used throughout the computations:

$$t(x) = c[a^{(1-x/l)} - 1] = c[s(x) - 1]. \tag{60}$$

The coordinate system of Fig. 1 is used here. The real part of $g(x)$ increases from a value $s(l)=1$ at the front surface $x=l$ to a maximum value $s(0)=a$ at the terminating wall $x=0$. The loss part $t(x)$ may have an initial step at $x=l$, if $d\neq 1$ in (59).

In Fig. 10 two solutions are plotted for comparison. The solid line represents the electromagnetic case of conductivity losses ($t\sim 1/\omega$) with a short-circuit termination. The dashed line corresponds to frequency independent losses. The differences between the two cases for small l/λ have been discussed in Section III-B, 2); also compare Fig. 7. The solid curve in Fig. 10 is very close to an example given by Lenz.[20] The l/λ cutoff values for $r\leq 10$ per cent are located between 0.35 and 0.40.

The solutions in Fig. 11 are to illustrate the electromagnetic case of a conductive layer with an open-circuit termination; compare Fig. 7, curve 4. The difficulties in realizing this case physically have been mentioned in Section III-B, 2). The curves in Fig. 11 start with finite r values for $l/\lambda=0$. Reflection factors below 10 per cent are not accomplished over a wide l/λ range for low frequencies. For low conductivities (solid line in Fig. 11), a fairly good impedance match can be achieved for $l/\lambda=0$; however, the attenuation for higher frequencies is insufficient (57). Therefore, the reflection factor increases with l/λ. Increasing the conductivity (dotted line in Fig. 11) lowers the reflection factor for higher frequencies; however, a severe mismatch is caused for small l/λ values.

Another interesting possibility of combining the principles of the Salisbury screen and the gradual-transition absorber has been pointed out by Deutsch and Thust.[21] These authors suggest placing a resistive foil in front of a gradual-transition absorber in order to extend the low-frequency absorption range by means of a resonance effect. Kurtze[22] was able to improve the low-frequency response of porous sound absorbers (wedge-type) by providing an air space between the wedges and the terminating wall.

In order to study the effect of highly refractive panels for the construction of gradual-transition absorbers, several numerical solutions of r have been calculated. These are shown as a function of the ratio l/λ in Figs. 12(a) through 18(b). Frequency independent material constants are assumed. The maximum values of $s(x)$ vary from 1 in Fig. 12 to 100 in Fig. 18. The parts (a) of Figs. 12 through 18 satisfy the boundary condition $R(0)=-1$. This case can be realized with electric losses and a short-circuit termination for electromagnetic waves. For parts (b) of Figs. 12 through 18 the boundary condition reads $R(0)=+1$. An example for waterborne sound waves can be realized with compressibility losses in front of a rigid wall. Some numerical solutions for this case have been reported by Miller,[10] describing linear transitions in material constants and other functions.

The results in Figs. 12(a) through 18(b) show that the smallest l/λ value for which $r\leq 10$ per cent is accomplished for the optimum case of Fig. 12(a) with $s(x)=1$ (see also Lenz[20]). For highly refractive panels (Figs. 16 through 18) oscillations due to multiple reflections are observed. The "wavelength" of these oscillations decreases with increasing $s(x)$, as we would expect. Narrow-band resonance absorption for some points can be accomplished. However, judged from the $r\leq 10$ per cent criterion, these curves look inferior to the result of Fig. 12(a). The general behavior of these curves has been discussed in detail in Section III-C of this paper. If only one loss mechanism is present [$f(x)=1$ in Figs. 12(a) through 18(b)], increasing the losses does not improve the performance of the absorber. The oscillations are damped out by this method, but the "average" level is raised at the same time (52).

An improvement in the performance of highly refractive panels can be achieved if two types of losses are present simultaneously (for instance, electric and magnetic losses). The difficulties for realizing the desired condition $f(x)=g(x)$ in absorber design for electromagnetic and acoustic waves are mentioned in the literature.[1,23] Pottel[23] points out some possibilities of realizing the condition $\epsilon=\mu$ for some anisotropic media in the microwave range. In artificial dielectric media both electric and magnetic losses are present simultaneously, although generally $|\epsilon|\gg|\mu|$ in the microwave range.[1,23–25] Porous materials for absorption of sound waves in air (for instance fiberglass) show high friction losses and a small component of compressibility losses.[26] Plastic materials are used in underwater sound absorption. Complex compressibilities and densities of the materials can be adjusted in wide ranges by either introducing cavities filled with different lossy materials or by loading the material with heavy, rigid obstacles, for instance metal disks, etc.[1,3,10,17,18]

[21] J. Deutsch and P. Thust, "Breitbandabsorber für elektromagnetische Wellen," *Z. angew Phys.*, vol. 11, pp. 453–455; December, 1959.

[22] G. Kurtze, "Untersuchungen zur Verbesserung der Auskleidung schallgedämpfter Räume," *Acustica*, vol. 2, Beiheft 2, pp. AB 104–AB 107; 1952.

[23] R. Pottel, "Absorption elektromagnetischer Zentimeterwellen in künstlich anisotropen Medien," *Z. angew. Phys.*, vol. 10, pp. 8–16; January, 1958.

[24] J. M. Kelly, J. O. Stenoien, and D. E. Isbell, "Waveguide measurements in the microwave region on metal powders suspended in paraffin wax," *J. Appl. Phys.*, vol. 24, pp. 258–261; March, 1953.

[25] E. Meyer, H. J. Schmitt, and H. Severin, "Dielektrizitätskonstante und Permeabilität künstlicher Dielektrika bei 3 cm Wellenlänge," *Z. angew. Phys.*, vol. 8, pp. 257–263; June, 1956.

[26] C. W. Kosten, "Behaviour of absorbing materials," in "Technical Aspects of Sound," E. G. Richardson, ed., Elsevier Publishing Co., New York, N. Y., vol. 1, ch. 4, pp. 49–104; 1953.

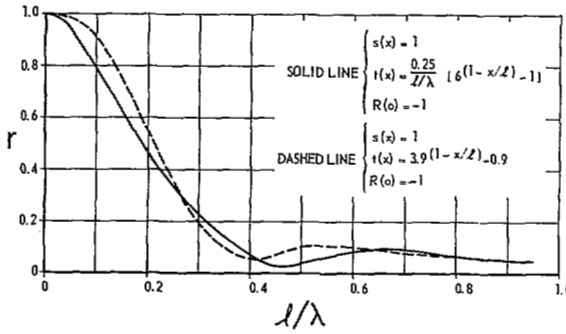

Fig. 10—Reflection factor r for layers with electric losses and short-circuit termination.
Solid line: ohmic conductivity losses with $t \sim \omega^{-1}$.
Dashed line: frequency independent electric losses.

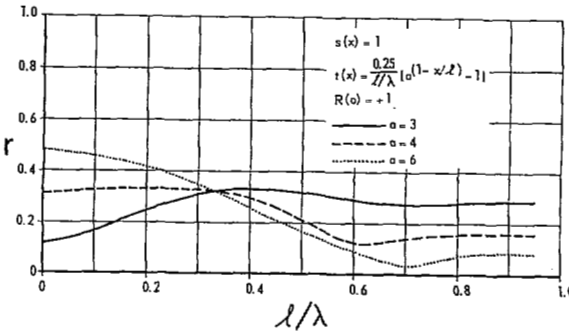

Fig. 11—Reflection factor r for layers with ohmic conductivity losses and open circuit termination.

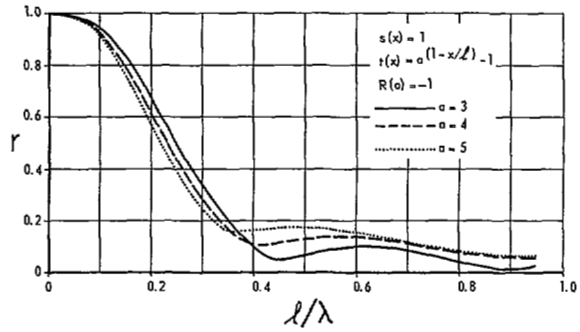

(a)

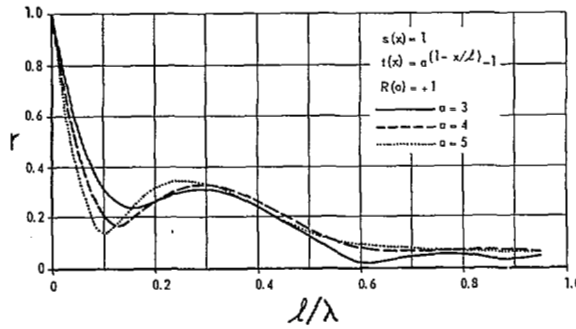

(b)

Fig. 12—Reflection factor r for layers with *one* type of frequency independent losses: $g(x) = s(x) - j \cdot t(x)$; $f(x) \equiv 1$. (a) Boundary condition $R(0) = -1$. (b) Boundary condition $R(0) = +1$.

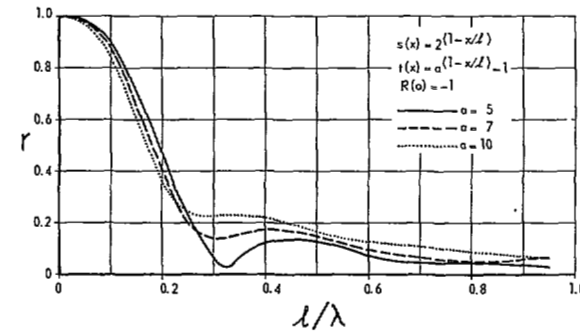

(a)

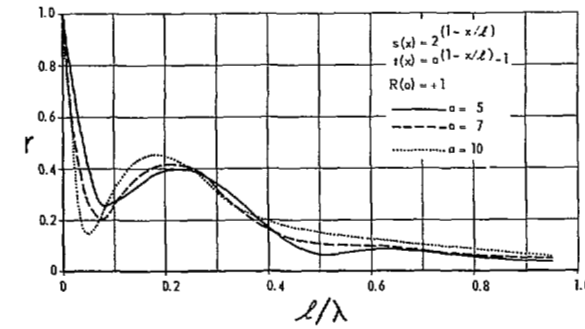

(b)

Fig. 13—Reflection factor r for layers with *one* type of frequency independent losses: $g(x) = s(x) - j \cdot t(x)$; $f(x) \equiv 1$. (a) Boundary condition $R(0) = -1$. (b) Boundary condition $R(0) = +1$.

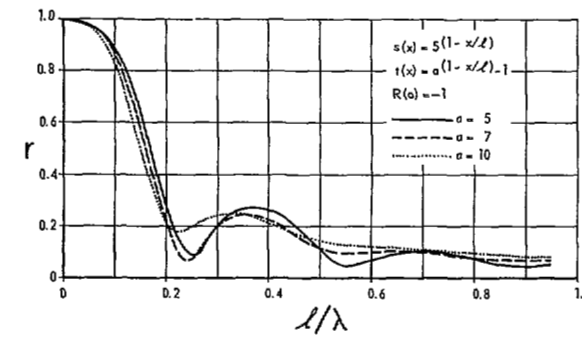

(a)

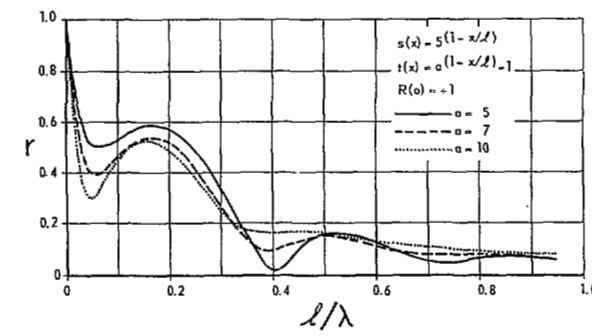

(b)

Fig. 14—Reflection factor r for layers with *one* type of frequency independent losses: $g(x) = s(x) - j \cdot t(x)$; $f(x) \equiv 1$. (a) Boundary condition $R(0) = -1$. (b) Boundary condition $R(0) = +1$.

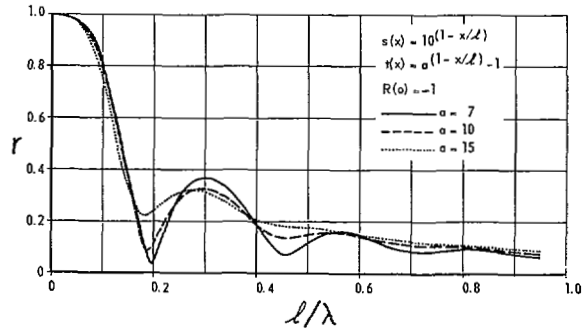

(a)

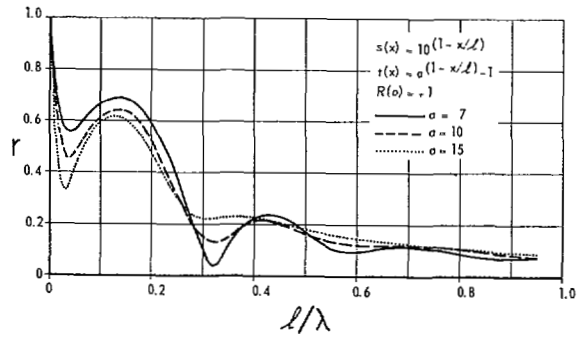

(b)

Fig. 15—Reflection factor r for layers with *one* type of frequency independent losses: $g(x)=s(x)-j\cdot t(x)$; $f(x)\equiv 1$. (a) Boundary condition $R(0)=-1$. (b) Boundary condition $R(0)=+1$.

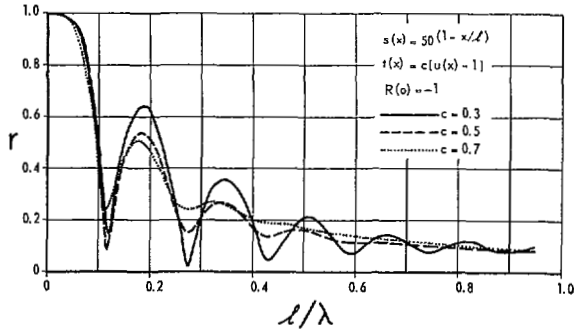

(a)

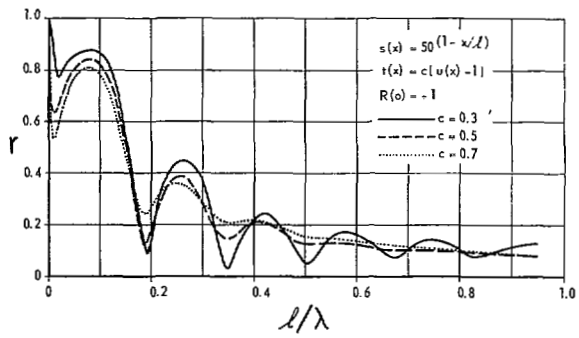

(b)

Fig. 17—Reflection factor r for layers with *one* type of frequency independent losses: $g(x)=s(x)-j\cdot t(x)$; $f(x)\equiv 1$. (a) Boundary condition $R(0)=-1$. (b) Boundary condition $R(0)=+1$.

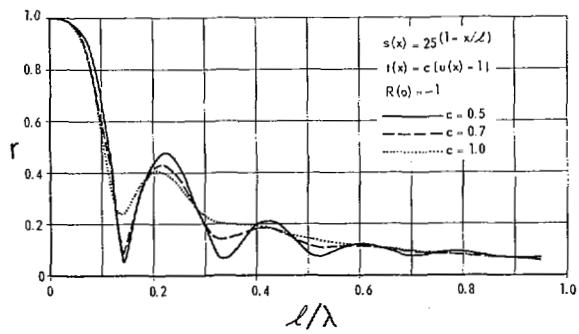

(a)

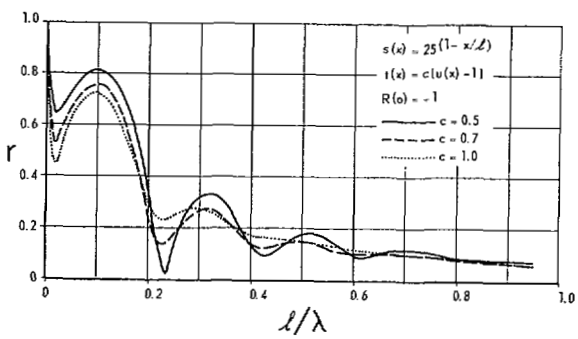

(b)

Fig. 16—Reflection factor r for layers with *one* type of frequency independent losses: $g(x)=s(x)-j\cdot t(x)$; $f(x)\equiv 1$. (a) Boundary condition $R(0)=-1$. (b) Boundary condition $R(0)=+1$.

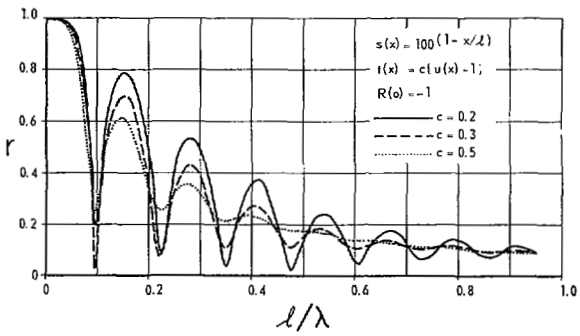

(a)

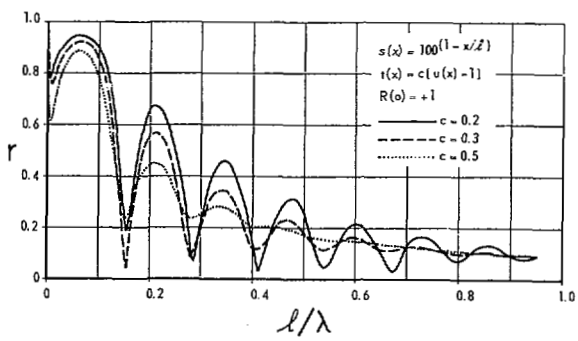

(b)

Fig. 18—Reflection factor r for layers with *one* type of frequency independent losses: $g(x)=s(x)-j\cdot t(x)\equiv 1$. (a) Boundary condition $R(0)=-1$. (b) Boundary condition $R(0)=+1$.

These examples illustrate that generally two types of losses can be realized simultaneously. However, either a condition $|f| \gg |g|$ or $|f| \ll |g|$ may prevail. Figs. 19(a) and 19(b) show that even under such conditions a considerable improvement in the performance of highly refractive panels can be achieved. For the microwave case, Fig. 19(a) may represent a panel with high real part of dielectric constant $s(0) = \epsilon'(0) = 50$ and a small real part $u(0) = \mu'(0) = 3.3$ in permeability. It can be seen that for increasing magnetic losses $v(x)$ the typical oscillations of Fig. 18 are damped out very rapidly. At the same time, the "average" level is *lowered*, since the tendency is to approach the condition $f(x) = g(x)$ in this case. Measurements of Pottel[23] on mixtures of paraffin and carbonyl iron powder at frequencies around 4 kmc show that the material constants of Fig. 19(a) can be realized approximately. It should be mentioned that for the calculations in Figs. 19(a) and 19(b) the material constants are assumed to be independent of frequency. In such artificial dielectrics, however, the magnetic losses vary with frequency according to a magnetic relaxation process.[27]

According to the criterion $r \leq 10$ per cent, the curves in Figs. 19(a) and 19(b) do not show advantages as compared to the results of Lenz[20] (see Fig. 10). If, however, somewhat higher reflection factors can be tolerated, for instance $r \leq 20$ per cent, the case of highly refractive panels in Fig. 19 shows a definite improvement over the case $s(x) = 1$ (Fig. 10).

Experimental results for the reflection factor of gradual-transition absorbers show that, in practice, smaller l/λ cutoff values for $r \leq 10$ per cent can be obtained than those predicted from theory. For wedge-type porous sound absorbers the condition $r \leq 10$ per cent can be realized for $l/\lambda \gtrsim 0.2$ or even slightly smaller values.[22,28] For commercially available microwave absorbers a similar situation prevails. Measurements by Haddenhorst[29] on dielectric wedge structures show that for lossless dielectrics with moderate ϵ' values a wedge structure can be adequately described by the theory of an equivalent inhomogeneous layer. We feel, however, that the one-dimensional theory of inhomogeneous layers is not completely satisfactory for describing the performance of highly absorbent wedge or pyramid structures. For these cases the exact two- or three-dimensional boundary value problems have to be solved in order to get a better agreement with the experimental results.

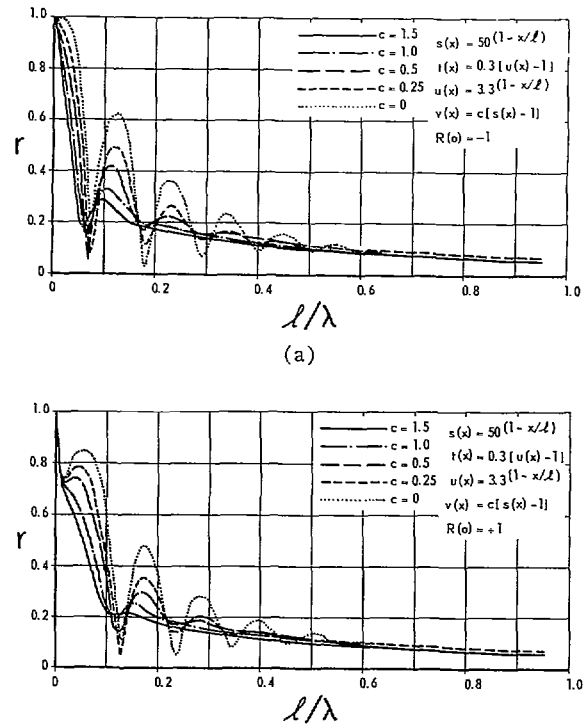

Fig. 19—Reflection factor r for layers with *two* types of frequency independent losses: $g(x) = s(x) - j \cdot t(x)$; $f(x) = u(x) - j \cdot v(x)$; $|f(x)| \ll |g(x)|$. (a) Boundary condition $R(0) = -1$. (b) Boundary condition $R(0) = +1$.

List of Symbols[30]

l = thickness of absorbing layer.
x, y, z = rectangular coordinates.
ξ = normalized length coordinate.
λ = wavelength in free propagation medium.
$k = 2\pi/\lambda$ = wave number.
ω = angular frequency.
$\Omega = (\omega/c)l$ = normalized frequency.
$c = \omega/k$ = phase velocity in free propagation medium.
$w_\nu(\xi)\,(\nu = 1, 2, 3)$ = weighting functions for thin absorbers.
$E(x)$ = electric field strength.
$H(x)$ = magnetic field strength.
$\epsilon(x) = \epsilon'(x) - j\epsilon''(x)$ = relative dielectric constant.
$\mu(x) = \mu'(x) - j\mu''(x)$ = relative permeability.
ϵ_0 = absolute dielectric constant of free space.
μ_0 = absolute permeability of free space.
$Z_0 = \sqrt{\mu_0/\epsilon_0}$ = electric wave impedance of free space.

[27] L. Lewin, "The electrical constants of a material loaded with spherical particles," *J. IEE*, pt. III, vol. 94, pp. 65–68; January, 1947.
[28] L. Z. Pronenko and A. N. Rivin, "Absorbent linings of glass staple fibre for an acoustic test chamber," *Soviet Phys. Acoustics*, vol. 5, pp. 387–388; February, 1960.
[29] H. G. Haddenhorst, "Durchgang von elektromagnetischen Wellen durch inhomogene Schichten," *Z. angew. Phys.*, vol. 7, pp. 487–496; October, 1955.

[30] Further symbols, which are used less frequently, are explained in the text.

$P(x)$ = sound pressure.
$V(x)$ = particle velocity.
$\kappa(x) = \kappa'(x) - j\kappa''(x)$ = relative compressibility.
$\rho(x) = \rho'(x) - j\rho''(x)$ = relative density.
κ_0 = absolute compressibility, ρ_0 = absolute density } of homogeneous medium.
$Z = \sqrt{\rho_0/\kappa_0}$ = acoustic wave impedance of homogeneous medium.
$Z(x)$ = general wave impedance.
$R(x)$ = "Redheffer"-reflection factor.
$R_s(x)$ = "Schelkunoff"-reflection factor.
$r(x) = |R(x)|$ = absolute amount of reflection factor.
$f(x) = u(x) - jv(x)$, $g(x) = s(x) - jt(x)$ } = loss functions in absorbing material.
Y_i/Y_o = normalized input admittance.
Z_i/Z_o = normalized input impedance.
σ = ohmic conductivity.
$R_\square$ = area-resistance.
$Y_\square = R_\square^{-1}$ = area-conductance.
"e" as a subscript = refers to the electromagnetic case.
"a" as a subscript = refers to the acoustic case.

ACKNOWLEDGMENT

Stimulating discussions with Dr. W. E. Kock and E. J. McGlinn on the general subject are appreciated. Assistance in numerical calculations was given by R. E. Lord and J. M. Patterson, supervisors of the Bendix Analog and Digital Computer Facility. The author especially wishes to acknowledge the cooperation of Mrs. P. A. Jacoby, who carried out most of the numerical runs on the Bendix analog computer.

A New Sporadic Layer Providing VLF Propagation*

J. ORTNER, A. EGELAND, AND B. HULTQVIST†

Summary—**During two periods in May and July, 1959, following strong solar flares, the signal strength of receptions at Kiruna of VLF transmissions from Rugby (16 kc) showed no or only slight diurnal variation. It is proposed that the change of the diurnal variation is due to the production by solar protons of an ionized layer very deep in the atmosphere, the electron density of which is sufficient for reflection of very long waves but too low to cause measurable nondeviative absorption in the HF band at geomagnetic latitudes lower than approximately 60°.**

INTRODUCTION

SOLAR flares are known to influence VLF propagation in several ways. One of the most spectacular effects of the ultraviolet radiation emitted by such flares is the "sudden phase anomaly" of VLF transmissions, first reported by Budden and Ratcliffe [12], which permits good timing of the arrival of the electromagnetic radiation upon the day side of the earth. The sudden ionospheric disturbance usually does not produce any appreciable change of amplitude on very low frequencies, at least over distances shorter than 1000 km [10], but there are indications that for waves reflected at oblique incidence, the reflection coefficient of the ionosphere is reduced during an SID for frequencies less than 10 kc [17], [9], and increased for frequencies greater than 10 kc [13].

* Received by the PGAP, June 30, 1960.
† Kiruna Geophys. Observatory of the Royal Swedish Academy of Science, Kiruna, Sweden.

Some of the evidence as to the effect on VLF propagation of the beams of corpuscular radiation emitted by solar flares, which produce magnetic storms, is inconclusive and in certain cases contradictory [24]. However, several workers agree that over transatlantic paths, the effect of a magnetic storm on VLF propagation is to reduce field strength at night and to increase it by day [16], [3], [4], [7]. In any case, the magnetic storm effect is not a spectacular one.

A very great effect on VLF propagation, of a kind never before observed [18], [15], was produced by the solar eruption of February 23, 1956.

Coinciding with the increase of cosmic ray intensity at about 0345 UT, a rapid diminution of the signal strength of atmospherics in the VLF and lower LF bands was observed by Aarons and Barron [1] (49 kc), Belrose, *et al.* [8] (22 kc), Ellison and Reid [15] (24 kc), Gold and Palmer [18] (27 kc), Ehmert and Revellio [14] (27 kc), and Lauter, *et al.* [25] (25, 35, and 40 kc). A similarly rapid and substantial decrease of the field strength of transmissions from Rugby (GBR, 16 kc) was found by Stoffregen [37] at Uppsala, Sweden; and an analogous phenomenon was recorded at Munich, Germany, by Schumann [34] for signals from the U. S. transmitter NSS (17.7 kc). At the same time, a sudden phase anomaly occurred in the receptions of GBR at Cambridge, England [8]. Allan, *et al.* [2] in New Zea-